A Feasibility analysis on using Bathymetry for Navigation of Autonomous Underwater Vehicles

ABSTRACT

Bathymetric terrain maps generated from acoustic data offer an attractive alternative for reducing the submerged pose error estimates for autonomous underwater vehicles (AUVs). The goal of this work is to determine the extent of improvement in the navigational accuracy of an AUV equipped with an echo sounder for near-seafloor, shallow water applications. Given bathymetric variations of a certain terrain, this paper analyzes the best achievable positioning accuracy for AUVs. To counter for the strong non-linearity and the non-Gaussian nature of the problem, an optimal Bayesian estimator is initially derived. It is then implemented using a Bayesian Bootstrap filter. The fundamental limitations in the pose uncertainty using this approach is encompassed by the Posterior Cramér-Rao bound (PCRB), that is interpreted in terms of the sonar sensor accuracy and the bathymetric variations. The PCRB on the position error covariance is determined and it is shown that the Bayesian Bootstrap filter closely follows this bound using real inferometric sonar data collected off the coast of Portsmouth. The results demonstrate that significant variations in the bottom topography of underwater terrain could be used to drastically improve the localization accuracy of the AUVs.

Keywords

Bathymetry aided navigation, AUV Localization, Bayesian Bootstrap filters, Posterior Cramer-Rao bounds, Underwater Robot navigation

1. INTRODUCTION

In most AUVs, underwater positioning is achieved by dead reckoning sensors such as Inertial Navigation System (INS) or Doppler Velocity Log (DVL). Regardless of the velocity aiding sensor and INS accuracy, the pose accuracy will eventually degrade necessitating position fixes. In some applications a GPS can be used to provide absolute position fixes to bound the drift. However under certain circumstances, surfacing to obtain GPS fixes may not be desirable due to efficiency or the nature of operation, prompting the need for alternate means of positioning underwater. Furthermore, absolute position fixes can also be provided by acoustic positioning systems like the Long Baseline (LBL), the Ultra Short Baseline (USBL), or the GPS equipped acoustic buoys [8]. However, these systems require an extensive surface support and also involve cumbersome deployments. Moreover, they constrain the area of operation as the transponders and the vehicle's receivers must be on line of sight at all times. In the last two decades, approaches that utilize the on-board exteroceptive sensors for AUV positioning (see fig. 1) have gained momentum in form of Map aided Localization (MAL) [3], [11],[10], [4] and Simultaneous Localization and Mapping (SLAM), [12], [5], [2], [13]. Both MAL and SLAM have a great potential to improve the autonomy of underwater vehicles, allowing them to position accurately without having to surface for GPS fixes and move beyond the acoustic coverage of the transponder networks.

This paper attempts to answer two fundamental questions: Given bathymetric variations of a underwater terrain, what is the best achievable positioning accuracy for the AUVs? How does larger bathymetric variations in the terrain affect the AUV localization performance? To resolve this, a bathymetry aided navigation (BAN) system is built around correcting the vehicle pose that takes advantage of existing ship-derived bathymetry map of the area of interest, where the AUV shall navigate. The strategy is to use ship-derived inferometric map of the underwater terrain as a corrective feedback against which AUV-derived bathymetry is compared - thereby, reducing the dead reckoning drift. This map matching problem is treated as a recursive non-linear estimation problem within the Bayesian framework. This leads to a family of recursive Bayesian methods referred to as Sequential Monte Carlo (SMC) filter. Section 2 describes this problem framework and its evaluation. To assess the accuracy of the filter and its performance, we derive a Posterior Cramér Rao Bound (PCRB) for the BAN system in section 3. Performance evaluation of the BAN system is presented in section 4. Finally, section 5 summarizes the paper and presents ideas for future work.

2. PROBLEM FRAMEWORK

The problem associated with bathymetric aided navigation is to match the AUV-derived bathymetry measurements with a ship-derived gridded bathymetric map. Fig. 1 shows an AUV that measures the bathymetry of the underwater terrain with a single beam at each sampling event. Let z_k be the bathymetric measurements taken by a sensor on-

Permission to make digital or hard copies of all or part of this work for personal or classroom use is granted without fee provided that copies are not made or distributed for profit or commercial advantage and that copies bear this notice and the full citation on the first page. To copy otherwise, to republish, to post on servers or to redistribute to lists, requires prior specific permission and/or a fee.

SAC'13 March 18-22, 2013, Coimbra, Portugal.

Copyright 2013 ACM 978-1-4503-1656-9/13/03 ...$10.00.

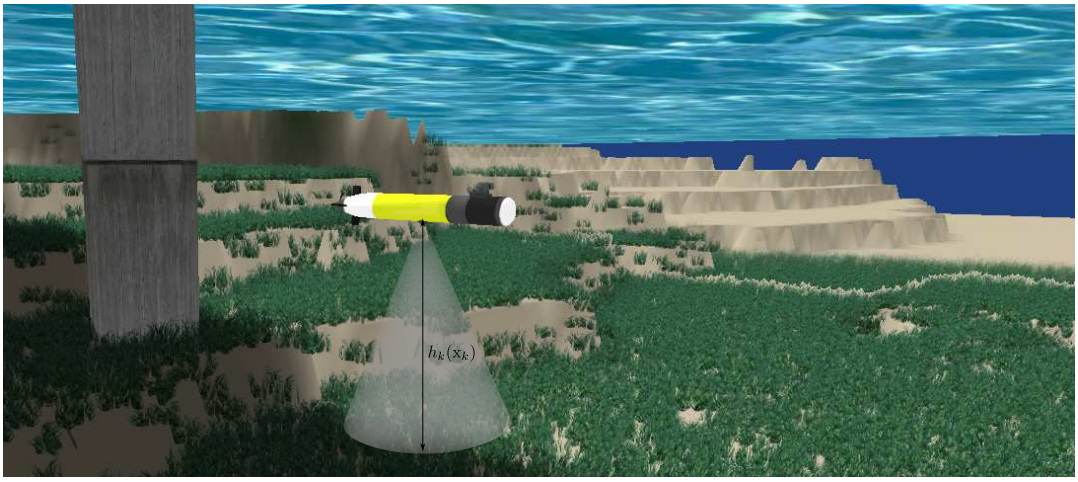

Figure 1: An illustration of the principle of Bathymetry aided underwater navigation using AUV. The AUV is equipped with an *apriori* bathymetry map of the area and an echo sounder that measures the range to bottom. The likely position of the AUV are positions in the bathymetry map with the same profiles.

board at time k. Let $\mathrm{Z}_k = [\mathrm{z}_1, \mathrm{z}_2, \ldots, \mathrm{z}_k]^T$ denote the history of all the measurements taken up to time k. Let $\mathrm{X}_k = [\mathrm{x}_1, \ldots, \mathrm{x}_k]$ denote the vehicle's complete state history, where $\mathrm{x}_k = [x_k, \dot{x}_k, y_k, \dot{y}_k]^T$. The vehicle motion model attempts to capture the fundamental relationship between the vehicle's past state x_{k-1} and its current state x_k and is modeled as,

$$\mathrm{x}_k = f_k(\mathrm{x}_{k-1}) + \mathrm{v}_{k-1} \tag{1}$$

where, $\mathrm{v}_{k-1} = \mathcal{N}(\mathrm{v}_{k-1}; 0, Q_{k-1})$ is assumed to be an additive Gaussian white noise. The measurement model relates the vehicle's position and the bathymetry measurements and is modeled as

$$\mathrm{z}_k = h_k(\mathrm{x}_k) + \mathrm{w}_k \tag{2}$$

where, $\mathrm{w}_k = \mathcal{N}(\mathrm{w}_k; 0, R_k)$ is assumed to be an additive Gaussian white noise. This additive noise models both the sensor measurement error and the error originating from an incorrect bathymetry map of the actual terrain.

2.1 The Bayesian approach to Recursive Estimation

From a Bayesian perspective the objective of bathymetry aided navigation is to recursively estimate some degree of belief in the state x_k from the series of bathymetry measurements Z_k. Thus, it is required to construct a posterior density function $p(\mathrm{x}_k \mid \mathrm{Z}_k)$ under the assumption of a known prior $p(\mathrm{x}_0)$. This can be obtained by a two step recursive process viz., time-update and measurement-update. The time-update step involves using the vehicle motion model as defined in (1) to obtain the prior pdf of the vehicle state at time k:

$$p(\mathrm{x}_k \mid \mathrm{Z}_{k-1}) = \int p(\mathrm{x}_k \mid \mathrm{x}_{k-1}) p(\mathrm{x}_{k-1} \mid \mathrm{Z}_{k-1}) d\mathrm{x}_{k-1} \tag{3}$$

The data-update step involves using the calculated prior density and sensor likelihood function as defined in the measurement model in (2) to obtain the required posterior density function via Bayes rule:

$$p(\mathrm{x}_k \mid \mathrm{Z}_k) = \frac{p(\mathrm{z}_k|\mathrm{x}_k) p(\mathrm{x}_k \mid \mathrm{Z}_{k-1})}{p(\mathrm{z}_k \mid \mathrm{Z}_{k-1})} \tag{4}$$

where,

$$p(\mathrm{z}_k \mid \mathrm{Z}_{k-1}) = \int p(\mathrm{z}_k \mid \mathrm{x}_k) p(\mathrm{x}_k \mid \mathrm{Z}_{k-1}) d\mathrm{x}_k \tag{5}$$

is a normalizing constant. Equations (3) and (4) provide a recursive procedure for calculating the posterior density and thus provide a Bayesian solution to the non-linear problem defined in (1)-(2). However, each iteration in (3)-(4) involves multiple integrals and given the highly non-linear nature of the measurement equation (2), it is impossible to obtain a closed form solution that solves the posterior density analytically. Few approaches have been proposed to mitigate this problem based on local linearizations such as Extended Kalman filter, Unscented Kalman filter [7] and numerical approximation techniques in form of Particle filters [9], [1]. In this paper, a Bayesian Bootstrap particle filter (also known as Sampling Importance Resampling (SIR) particle filer) is used[1].

The main idea behind this approach is to approximate the posterior density function $p(\mathrm{x}_k \mid \mathrm{Z}_k)$ by a set of random samples $\{\mathrm{x}_k^{[i]}, w_k^{[i]}\}_{i=1}^{N_s}$, where $\{\mathrm{x}_k^{[i]}\}$ is a set of support points with their associated weights $\{w_k^{[i]}\}$. The weights are normalized such that $\sum_i w_k^{[i]} = 1$. Given a proposal distribution (importance) function $q_k(\cdot|\mathrm{x}_{k-1}^{[i]}, \mathrm{Z}_k)$, the SMC filter approximates the posterior at time k by a set of weighted particles $\{\mathrm{x}_k^{[i]}, w_k^{[i]}\}_{i=1}^{N_s}$ i.e.,

$$p(\mathrm{x}_k|\mathrm{Z}_k) \approx \sum_{i=1}^{N_s} \tilde{w}_k^{[i]} \delta(\mathrm{x}_k - \mathrm{x}_k^{[i]}) \tag{6}$$

where,

$$\mathrm{x}_k^{[i]} \sim q_k(\mathrm{x}_k|\mathrm{x}_{k-1}^{[i]}, \mathrm{Z}_k) \tag{7}$$

$$w_k^{[i]} = w_{k-1}^{[i]} \frac{p(\mathrm{Z}_k|\mathrm{x}_k^{[i]}) p(\mathrm{x}_k^{[i]}|\mathrm{x}_{k-1}^{[i]}}{q_k(\mathrm{x}_k|\mathrm{x}_{k-1}^{[i]}, \mathrm{Z}_k)} \tag{8}$$

$$\tilde{w}_k^{[i]} = w_k^{[i]} / \sum_{j=1}^{N_s} w_k^{[j]}, i = 1, \ldots, N_s \quad (9)$$

The basic particle filter described above is well known to be subjected to degeneracy phenomenon, where after a few iterations, all but one particle will have negligible weight. In [1], it has also been shown that the variance of the importance weight increases with time, thereby making it difficult to avoid the degeneracy phenomenon. However, this phenomenon is usually overcome with a proper choice of proposal distribution function and the use of re-sampling techniques. Several re-sampling techniques have been developed as discussed in [1]. In this paper, SIR technique is adopted for its effectiveness in minimizing the sample variation [9].

3. THE POSTERIOR CRAMÉR-RAO BOUND FOR BATHYMETRY AIDED NAVIGATION

The Posterior Cramér-Rao bound (PCRB) sets a fundamental limit on the achievable algorithm performance. It sets the lower limit on the error covariance matrix of an unbiased estimator that is calculated from the Fisher information matrix (FIM). This can be used to evaluate the performance of the earlier discussed Bootstrap particle filter that solves the non-linear BAN problem. We now derive the expressions for the PCRB for the BAN problem, and more specifically under a Gaussian additive noise assumption.

The PCRB sets a lower limit on the mean square error (MSE) of an estimator. i.e.,

$$P_k \triangleq E\left[[\hat{g}_k(\mathrm{z}_k) - \mathrm{x}_k][\hat{g}_k(\mathrm{z}_k) - \mathrm{x}_k]^T\right] \geq \mathcal{J}_k^{-1} \quad (10)$$

where, $\hat{g}_k(\mathrm{z}_k)$ is an estimate of x_k, P_k is the PCRB on the estimation error, $\mathcal{J}$ is a $r \times r$ Fisher Information Matrix (FIM) with[1]

$$\mathcal{J}_{ij} = E\left[-\frac{\partial^2 \log p(\mathrm{z},\mathrm{x})}{\partial \mathrm{x}_i \partial \mathrm{x}_j}\right] \qquad i,j = 1 \ldots r, \quad (11)$$

provided the expectations and the derivatives in (10) and (11) exist.

Let ∇ be the first order partial derivative such that

$$\nabla_{\mathrm{x}} = \left[\frac{\partial}{\partial \mathrm{x}_1}, \ldots, \frac{\partial}{\partial \mathrm{x}_r}\right]^T \quad (12)$$

$$\Delta_{\Psi}^{\mathrm{x}} = \nabla_{\Psi} \nabla_{\mathrm{x}}^T \quad (13)$$

Using this notation, (11) can be written as

$$\mathcal{J} = E\left[-\Delta_{\mathrm{x}}^{\mathrm{x}} \log p(\mathrm{z},\mathrm{x})\right] \quad (14)$$

Since $p(\mathrm{z},\mathrm{x}) = p(\mathrm{z} \mid \mathrm{x}) f(\mathrm{x})$, $\mathcal{J}$ can be decomposed into two additive parts

$$\mathcal{J} = \mathcal{J}_D + \mathcal{J}_P \quad (15)$$

where, $\mathcal{J}_D$ represents the information obtained from the data, and $\mathcal{J}_P$ represents the *a priori* information.

Also $p(\mathrm{z},\mathrm{x}) = p(\mathrm{x} \mid \mathrm{z}).p(\mathrm{z})$. Since $p(\mathrm{z})$ is an integral $p(\mathrm{z},\mathrm{x})$ over x, it does not depend any longer on x; therefore, we have

$$\mathcal{J} = E\left[-\Delta_{\mathrm{x}}^{\mathrm{x}} \log p(\mathrm{x} \mid \mathrm{z})\right] \quad (16)$$

[1]Subscript k is dropped for notational convenience.

If we assume that x can be partitioned into two parts as $\mathrm{x} = [\mathrm{x}_\alpha^T, \mathrm{x}_\beta^T]^T$, then the FIM $\mathcal{J}$ can be correspondingly partitioned as follows

$$\mathcal{J} = \begin{bmatrix} \mathcal{J}_{\alpha\alpha} & \mathcal{J}_{\alpha\beta} \\ \mathcal{J}_{\beta\alpha} & \mathcal{J}_{\beta\alpha} \end{bmatrix} \quad (17)$$

It is shown that the covariance of estimation of x_β, P_β, is lower bounded by the lower right block of $\mathcal{J}^{-1}$[14],

$$\begin{aligned} P_\beta &\triangleq E\left[[\hat{g}_\beta(\mathrm{z}) - \mathrm{x}_\beta][\hat{g}_\beta(\mathrm{z}) - \mathrm{x}_\beta]^T\right] \\ &\geq \left[\mathcal{J}_{\beta\beta} - \mathcal{J}_{\beta\alpha}\mathcal{J}_{\alpha\alpha}^{-1}\mathcal{J}_{\alpha\beta}\right] \\ &= \mathcal{J}^{-1}(\mathrm{x}_\beta) \end{aligned} \quad (18)$$

provided $\mathcal{J}_{\alpha\alpha}^{-1}$ exists. The matrix $\mathcal{J}(\mathrm{x}_\beta)$ is called the information sub-matrix for x_β.

Given the non-linear model in described in (1) - (2), the total joint probability density function is given by

$$p(\mathrm{X}_k, \mathrm{Z}_k) = p(\mathrm{x}_0) \prod_{i=1}^{k} p(\mathrm{z}_i \mid \mathrm{x}_i) \prod_{j=1}^{k} p(\mathrm{x}_k \mid \mathrm{x}_{k-1}) \quad (19)$$

where $p(\mathrm{x}_0)$ is assumed to be known. From (14), we can derive the information matrix $\mathcal{J}(X_k)$ from the joint distribution $p(\mathrm{X}_k, \mathrm{Z}_k)$. Decomposing X_k as $\mathrm{X}_k = [\mathrm{X}_{k-1}, \mathrm{x}_k]^T$ and correspondingly $\mathcal{J}(\mathrm{X}_k)$ as

$$\begin{aligned} J(\mathrm{X}_k) &= \begin{bmatrix} A_k & B_k \\ B_k^T & C_k \end{bmatrix} \\ &\triangleq \begin{bmatrix} E\left[-\Delta_{\mathrm{X}_{k-1}}^{\mathrm{X}_{k-1}} \log p(\mathrm{X}_k, \mathrm{Z}_k)\right] & E\left[-\Delta_{\mathrm{X}_{k-1}}^{\mathrm{x}_k} \log p(\mathrm{X}_k, \mathrm{Z}_k)\right] \\ E\left[-\Delta_{\mathrm{x}_k}^{\mathrm{X}_{k-1}} \log p(\mathrm{X}_k, \mathrm{Z}_k)\right] & E\left[-\Delta_{\mathrm{x}_k}^{\mathrm{x}_k} \log p(\mathrm{X}_k, \mathrm{Z}_k)\right] \end{bmatrix}, \end{aligned} \quad (20)$$

provided the expectations and the derivatives exist. However, the problem we wish to solve is the computation of the information sub-matrix for estimating x_k, $\mathcal{J}(\mathrm{x}_k)$ (henceforth denoted as $\mathcal{J}_k$) which is given as the inverse of lower right block of $\mathcal{J}(\mathrm{X}_k)^{-1}$. This matrix will provide the lower bound on the mean square error of estimating x_k. Comparing (17) and (18) with (20) gives

$$\mathcal{J}_k = C_k - B_k^T A_k^{-1} B_k. \quad (21)$$

Given $\mathcal{J}_k$ and x_{k+1}, the desired recursive update equation for the information sub-matrix $\mathcal{J}(\mathrm{x}_{k+1})$ (henceforth denoted as $\mathcal{J}_{k+1}$ is shown to be [14]

$$\mathcal{J}_{k+1} = \Omega_k + D_k^{22} - D_k^{21}[\mathcal{J}_k + D_k^{11}]^{-1} D_k^{12} \quad (22)$$

where,

$$D_k^{11} = E\left[-\Delta_{\mathrm{x}_k}^{\mathrm{x}_k} \log p(\mathrm{x}_{k+1} \mid \mathrm{x}_k)\right] \quad (23a)$$

$$D_k^{12} = E\left[-\Delta_{\mathrm{x}_k}^{\mathrm{x}_{k+1}} \log p(\mathrm{x}_{k+1} \mid \mathrm{x}_k)\right] \quad (23b)$$

$$D_k^{21} = E\left[-\Delta_{\mathrm{x}_{k+1}}^{\mathrm{x}_k} \log p(\mathrm{x}_{k+1} \mid \mathrm{x}_k)\right] \quad (23c)$$

$$D_k^{22} = E\left[-\Delta_{\mathrm{x}_{k+1}}^{\mathrm{x}_{k+1}} \log p(\mathrm{x}_{k+1} \mid \mathrm{x}_k)\right] \quad (23d)$$

$$\Omega_k = E\left[-\Delta_{\mathrm{x}_{k+1}}^{\mathrm{x}_{k+1}} \log p(\mathrm{z}_{k+1} \mid \mathrm{x}_{k+1})\right] \quad (23e)$$

Further, with the additive Gaussian noise assumptions in (1) and(2) it follows that,

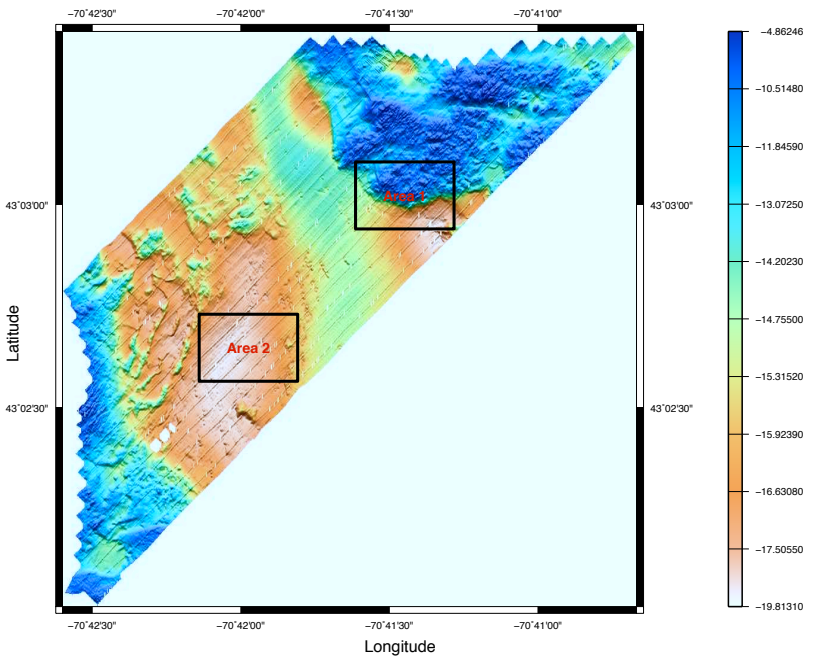

Figure 2: A Ship-derived bathymetry map around Portsmouth area. Overlaid in the foreground are the two patches of interest (area 1 and area 2) where the AUV performs a lawn mover pattern. (The bathymetry map was constructed using MB-System[6])

$$-\log p(\mathrm{x}_{k+1} \mid \mathrm{x}_k) = c_1 + \frac{1}{2}\left[[\mathrm{x}_{k+1} - f_k(\mathrm{x}_k)]^T Q_k^{-1} [\mathrm{x}_{k+1} - f_k(\mathrm{x}_k)]\right] \quad (24)$$

$$-\log p(\mathrm{z}_{k+1} \mid \mathrm{x}_{k+1}) = c_2 + \frac{1}{2}\left[[\mathrm{z}_{k+1} - h_{k+1}(\mathrm{x}_{k+1})]^T R_{k+1}^{-1} [\mathrm{z}_{k+1} - h_{k+1}(\mathrm{x}_{k+1})]\right] \quad (25)$$

where c_1 and c_2 are constants. This further simplifies (23) as follows:

$$D_k^{11} = E\left[[\nabla f_k(\mathrm{x}_k)]\, Q_k^{-1}\, [\nabla f_k(\mathrm{x}_k)]^T\right] \quad (26a)$$

$$D_k^{12} = -E\left[[\nabla f_k(\mathrm{x}_k)]\right] Q_k^{-1} = D_k^{21} \quad (26b)$$

$$D_k^{22} = Q_k^{-1} \quad (26c)$$

$$\Omega_k = E\left[[\nabla h_{k+1}(\mathrm{x}_{k+1})]\, .R_{k+1}^{-1}\, [\nabla h_{k+1}(\mathrm{x}_{k+1})]^T\right]. \quad (26d)$$

It can be seen that from (22) the PCRB $\mathcal{P}_{k+1} = [\mathcal{J}_{k+1}]^{-1}$ on the estimation error is only dependent on the noise parameters v_k and w_k introduced into the system (eqn. (1) and(2)). It is also influenced by the amount of information provided by the measurement z_k about x_k, which is also determined by the system in (2). The results of (26) define most of the variables (D_k^{11},D_k^{12} and D_k^{22}) required for a computation of the PCRB. However in the eq. (26d), the term $h_{k+1}(\cdot)$ is a non-linear function, part of the measurement model defined in (2). Hence the expectations in (26d) are computed as Monte Carlo runs over a series of realizations as follows: M independent tracks are generated at every time instance k to obtain a sequence $\left\{\mathrm{x}_k^{[i]}\right\}_{i=1}^{M}$. For every sample the local gradient $\left[\nabla h_{k+1}(\mathrm{x}_{k+1}^{[i]})\right]$ and the map covariance matrix $R_{k+1}^{[i]}$ is computed. The Ω_k in (26d) is thus computed by averaging the terrain gradient over all the M tracks.

4. PERFORMANCE EVALUATION OF THE BAN SYSTEM

The primary purpose of these experiments was to evaluate the feasibility and performance of bathymetric aided navigation under varying terrain characteristics. To achieve this, a conservative vehicle uncertainty bound is calculated based on PCRB (as derived in 3), and thereby determining the best achievable AUV pose accuracy for a given terrain patch. The ship-derived data was collected on the outer harbor of Portsmouth, NH, at the mouth of the Piscataqua river and the immediate near-shore area. The terrain in this area has a varying topography with mixed sand and rock seafloor, rock outcrops and other navigation significant features. The bathymetry data (refer fig. 2) was collected using a Sea SwathPlus inferometric sonar operating at 234kHz in conjunction with a CodaOctopus F180-R which is an attitude and position sensor.

To test the feasibility and performance of bathymetry aided navigation system for different terrain characteristics, two varying terrain patches were considered, one over a rocky sea floor with a bottom topography varying $\sim$ 5m (area 1 in fig. 2), and a smooth sandy patch with a bottom topography varying $\sim$ 2m (area 2 in fig. 2). A lawn mover pattern was performed to emulate an AUV traversing in these terrain patches as shown in fig. 3. The initial

vehicle state covariance is,

$$Q_0 = \begin{bmatrix} \sigma_x^2 & 0 & 0 & 0 \\ 0 & \sigma_{\dot{x}}^2 & 0 & 0 \\ 0 & 0 & \sigma_y^2 & 0 \\ 0 & 0 & 0 & \sigma_{\dot{y}}^2 \end{bmatrix} \tag{27}$$

where $\sigma_x = \sigma_y = 1000$m and $\sigma_{\dot{x}} = \sigma_{\dot{y}} = 0.1$m/s. The Bootstrap particle filter was initialized by $N_s = 50000$ particles, however, after a few iterations it reduced to under 3000. For the computation of the PCRB, $M = 2000$ independent tracks were generated.

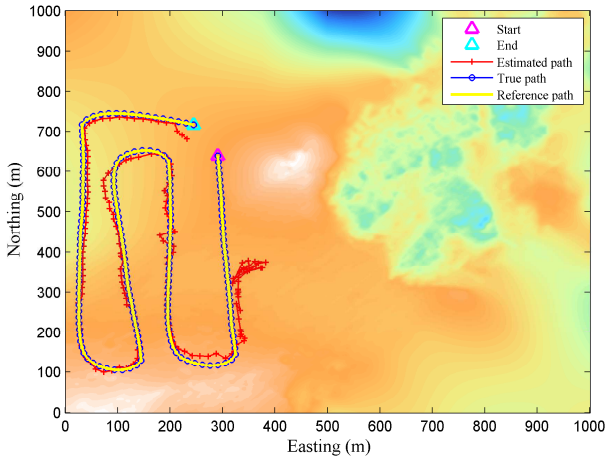

(a) AUV tracks along with the estimates are overlaid over a smooth sandy bathymetry patch

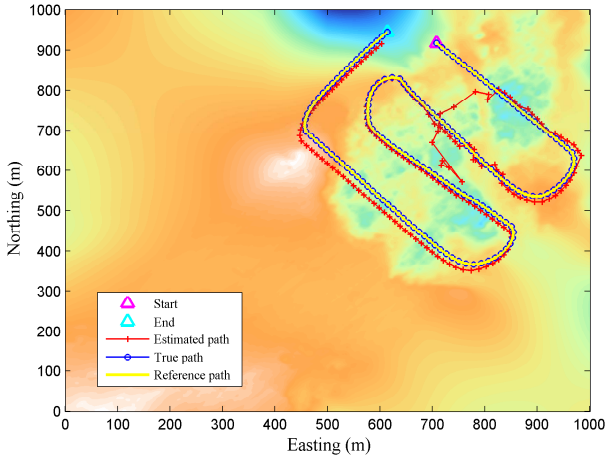

(b) AUV tracks along with the estimates are overlaid over a rocky bathymetry patch

Figure 3: A comparison of actual AUV tracks vs. the bathymetry aided navigation filter estimates for varying terrain patches.

The results of bathymetry aided navigation system using Bootstrap particle filter are shown in fig. 3 and fig. 4 for varying terrain patches. The results show that navigation filter conforms to the PCRB, and as expected, depends strongly on the variation of the bottom topography $h(\cdot)$. In the rocky bathymetry patch (area 1 in fig. 2), the RMS error is lower than smooth sandy bathymetry patch (area 2 in fig. 2) and the convergence rate is very close to the PCRB as seen 4. The vehicle pose error converges rapidly from initial error of 1km down to an error less than 5m.

5. CONCLUSION

This paper described a method for improving the localization accuracy of an AUV using bathymetry variations in the terrain. A conservative vehicle uncertainty bound was examined by calculating the PCRB, and thereby determining the maximum achievable AUV pose accuracy. Using this bound as reference, a Bayesian bootstrap filter was designed that provided an approximate solution to the non-linear problem in bathymetry aided navigation. They have demonstrated a near optimal performance as they closely conform with the PCRB. A strong correlation between localization accuracy and variation of bottom topography was established. Thus the approach has showed promise, particularly in areas of varying bottom topography.

Work is underway to formulate a featureless SLAM framework that would obviate the need for *apriori* maps. However, if *apriori* maps are available combining MAL with SLAM framework would be desirable. Furthermore, a higher level path planning algorithm can be implemented on the AUV to generate trajectories such that it operates in areas of larger terrain gradients.

6. ACKNOWLEDGMENT

The authors like to thank Brian Calder from Center for Coastal and Ocean Mapping, University of New Hampshire for providing the shallow water bathymetry data and Paul Byham from Bythymetry Consulting for providing the SEASwath-Plus sonar software.

7. REFERENCES

[1] A.Doucet, N. Freitas, and N.J.Gordon. *Sequential Montecarlo Methods in Practice*. Springer, 2001.

[2] S. Barkby, S. B. Williams, O. Pizarro, and M. V. Jakuba. A featureless approach to efficient bathymetric SLAM using distributed particle mapping. *J. Field Robot.*, 28(1):19 – 39, Jan. 2011.

[3] N. Bergman and L. Ljung. Point-mass filter and Cramer-Rao bound for terrain-aided navigation. In *Decision and Control, 1997., Proceedings of the 36th IEEE Conference on*, volume 1, pages 565 –570 vol.1, Dec. 1997.

[4] S. Carreno, P. Wilson, P. Ridao, and Y. Petillot. A survey on terrain based navigation for AUVs. In *OCEANS 2010*, pages 1 –7, Sept. 2010.

[5] H. Durrant-Whyte and T. Bailey. Simultaneous localization and mapping: part i the essential algorithms. *Robotics & Automation Magazine, IEEE*, 13(2):99 – 110, 2006.

[6] R. Henthorn, D. Caress, H. Thomas, R. McEwen, W. Kirkwood, C. Paull, and R. Keaten. High-Resolution multibeam and subbottom surveys of submarine canyons, Deep-Sea fan channels, and gas seeps using the MBARI mapping AUV. In *OCEANS 2006*, pages 1 – 6, Sept. 2006.

[7] S. Julier and J. Uhlmann. A new extension of the kalman filter to nonlinear systems. In *Int. Symp. Aerospace/Defense Sensing, Simul. and Controls, Orlando, FL*, 1997.

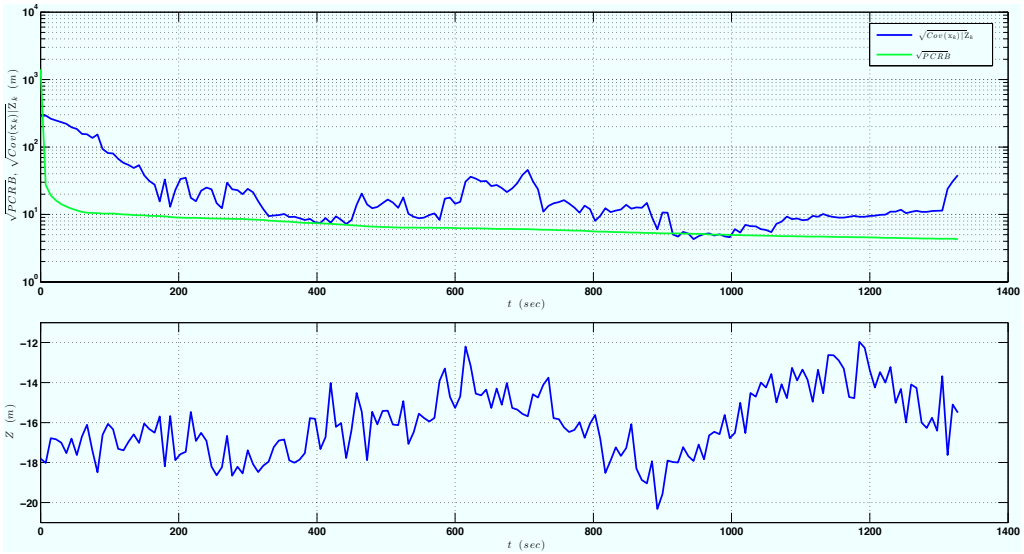

(a) For smooth sandy bathymetry patch

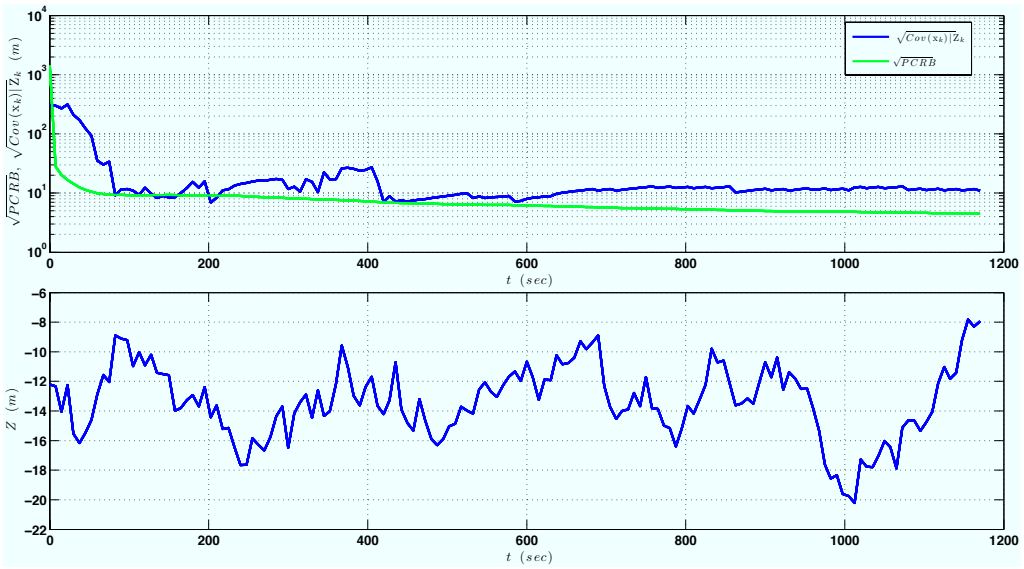

(b) For rocky bathymetry patch

Figure 4: A comparison of accuracy and convergence of the bathymetry aided navigation for varying terrain patches.

[8] J. C. Kinsey, R. M. Eustice, and L. L. Whitcomb. Underwater vehicle navigation: recent advances and new challenges. In *IFAC Conf. on Manoeuvring and Control of Marine Craft*, 2006.

[9] M.S.Arulampalam, S.Maskell, N.Gordon, and T.Clapp. A tutorial on particle filters for online nonlinear/non-Gaussian baysian tracking. *IEEE Transactions on Signal Processing*, 50(2), Feb. 2002.

[10] I. Nygren and M. Jansson. Terrain navigation for underwater vehicles using the correlator method. *IEEE Journal of Oceanic Engineering*, 29(3):906–915, July 2004.

[11] S. Paris and J. Le Cadre. Planning for terrain-aided navigation. In *Information Fusion, 2002. Proceedings of the Fifth International Conference on*, volume 2, pages 1007 – 1014 vol.2, 2002.

[12] C. Roman and H. Singh. Improved vehicle based multibeam bathymetry using sub-maps and SLAM. In *Intelligent Robots and Systems, 2005. (IROS 2005)*, pages 3662 – 3669, Aug. 2005.

[13] R. Stuckey. Navigational error reduction of autonomous underwater vehicles with selective bathymetric SLAM. In *IFAC Workshop - Navigation, Guidance & Control of Underwater Vehicles.*, 2012.

[14] P. Tichavsky, C. Muravchik, and A. Nehorai. Posterior Cramer-Rao bounds for discrete-time nonlinear filtering. *Signal Processing, IEEE Transactions on*, 46(5):1386 –1396, May 1998.